SHORT COMMUNICATION

Inhibition of MEK signaling prevents SARS-CoV2-induced lung damage and improves the survival of infected mice

Jingwu Xie[1] | Michael J. Klemsz[2] | Melissa A. Kacena[3] | George Sandusky[4] | Xiaoli Zhang[2] | Mark H. Kaplan[2]

[1]Department of Pediatrics, The Wells Center for Pediatrics Research, Indiana University School of Medicine, Indianapolis, Indiana, USA

[2]Department of Microbiology and Immunology, Indiana University School of Medicine, Indianapolis, Indiana, USA

[3]Department of Orthopaedic Surgery, Indiana University School of Medicine, Indianapolis, Indiana, USA

[4]Department of Pathology and Laboratory Medicine, Indiana University School of Medicine, Indianapolis, Indiana, USA

Correspondence
Jingwu Xie, Department of Pediatrics, The Wells Center for Pediatrics Research, Indiana University School of MedicineIndianapolis, IN 46202, USA.
Email: jinxie@iu.edu and jwx19631019@gmail.com

Funding information
National Institutes of Health; Indiana University

Abstract

Coronavirus disease 2019 (COVID-19) is the illness caused by severe acute respiratory syndrome coronavirus 2 (SARS-CoV-2). Over 500 million confirmed cases of COVID-19 have been recorded, with six million deaths. Thus, reducing the COVID-19-related medical burden is an unmet need. Despite a vaccine that is successful in preventing COVID-19-caused death, effective medication to relieve COVID-19-associated symptoms and alleviate disease progression is still in high demand. In particular, one in three COVID-19 patients have signs of long COVID syndrome and are termed, long haulers. At present, there are no effective ways to treat long haulers. In this study, we determine the effectiveness of inhibiting mitogen-activated protein kinase (MEK) signaling in preventing SARS-CoV-2-induced lung damage in mice. We showed that phosphorylation of extracellular signal-regulated kinase, a marker for MEK activation, is high in SARS-CoV-2-infected lung tissues of mice and humans. We also showed that selumetinib, a specific inhibitor of the upstream MEK kinases, reduces cell proliferation, reduces lung damage following SARS-CoV-2 infection, and prolongs the survival of the infected mice. Selumetinib has been approved by the US Food and Drug Administration to treat cancer. Further analysis indicates that amphiregulin, an essential upstream molecule, was upregulated following SARS-CoV-2 infection. Our data suggest that MEK signaling activation represents a target for therapeutic intervention strategies against SARS-CoV-2-induced lung damage and that selumetinib may be repurposed to treat COVID-19.

KEYWORDS

COVID-19, ERK phosphorylation, Ki67, lung, MEK, mouse model, SARS-CoV-2

1 | INTRODUCTION

Common symptoms of coronavirus disease 2019 (COVID-19) include fever, fatigue, and dry cough, occurring in most patients. In contrast, severe symptoms such as pneumonia, acute respiratory distress syndrome, and multiple organ failure are less common.[1–4] Effective medication to relieve COVID-19-associated symptoms and slow disease progression is an unmet medical need, despite vaccination successfully reducing severe symptoms and mortality rate. Direct targeting antivirals (DTA) such as remdesivir or monoclonal antibodies are more effective in the early stages of COVID-19, but ineffective in reducing late-stage symptoms. Increasing evidence indicates that both vaccination and DTA are not effective in combating illness caused by recent severe acute respiratory syndrome coronavirus 2 (SARS-CoV-2) variants.

We hypothesize that targeting cellular factors required for symptom development after SARS-CoV-2 infection will allow us to identify novel strategies to relieve COVID-19-associated symptoms, including those in long haulers. Over the years, it has been shown that activation of the RAF/MEK/ERK signaling pathway is critical for the replication of DNA[5,6] and RNA viruses, including SARS-CoV-2.[7–9] In this study, we demonstrated that selumetinib, a specific inhibitor of the upstream mitogen-activated protein kinases (MEK kinases), approved by the US Food and Drug Administration (FDA) for cancer treatments, prevents phosphorylation of extracellular signal-regulated kinase (ERK), and reduces lung damage following SARS-CoV-2 infection, and prolongs the survival of infected mice. Thus, repurposing selumetinib may be a promising approach to reducing COVID symptoms and pathology.

2 | MATERIALS AND METHODS

2.1 | Mouse model of SARS-CoV-2 infection

The Indiana University School approved all animal studies of the Institutional Animal Care and Use Committee (IACUC) and the Indiana University Institutional Biosafety Committee. Cg-Tg(K18-ACE2)2Prlmn/J mice (Stock No: 034860; Jackson Laboratory) were used in this study. At approximately 8 weeks of age, K18-ACE2 mice were either mock infected (media only) or were infected (media containing virus) intranasally (20 μl) with SARS-CoV-2 isolate USA-WA1/2020 (BEI Resources), ($n = 4–5$/group) using methods described previously.[10,11] Mice were administered with a viral concentration of 0 (mock) or 1×10^4 (plaque-forming unit). As detailed below, several additional assessments were also completed each day, including body weight and body condition score (BCS). Criteria for humane endpoints were established in consultation with IACUC and collaborating veterinarians as described previously.[11]

Discarded human specimens from COVID-19 patients were used to detect the expression of ERK[1/2] phosphorylation. The use of human materials has been approved by Institutional Review Board. We conducted the study after receiving institutional ethical committee clearance.

2.2 | Body condition scoring

BCS was performed as previously described[11] (see Table below). Mice with a score of 0–7 will continue with daily scoring. Mice with a score of 8 or greater or any category of a score of 3 will be euthanized.

Score	Activity	Posture	Respiration
0	Normal	Normal	Normal
1	Slightly reduced/mild gait abnormality	Slightly hunched	Slight increase in rate or effort
2	Moving very slowly/ severely altered gait	Moderately hunched	Slight to moderate increase in rate and/or effort
3	Reluctant to move or did not move	Severely hunched	Noticeable increase in rate and/or effort

2.2.1 | Virus preparation

SARS-CoV-2 isolate USA-WA1/2020 was propagated in Vero-furin cells, and progeny virions were collected in the supernatant 2–3 days postinfection. Vero-furin cells were used for virus production (Dulbecco's modified Eagle's medium supplemented with 10% fetal bovine serum and 1% penicillin–streptomycin at 37°C with 5% CO_2). SARS-CoV-2 was quantified by a plaque assay as previously described.[11]

2.2.2 | Histology and immunofluorescent staining

All mice were either euthanized at Day 14 ± 5 days or found dead, and lung tissues were placed in 10% NBF for at least 72 h as per the CDC-recommended guidelines. They were paraffin-embedded, sectioned, stained with hematoxylin and eosin stain (H&E), and examined by pathologist Dr. George Sandusky. Immunofluorescent staining was performed as described previously.[12] Antigen retrieval was performed with tissue sections from mouse and human COVID-19 lung tissues. Nonspecific staining was blocked with 10% FBS in PBS for 30 min and was then incubated with anti-phosphor-ERK[1/2] (1:100, cat# 4376 S, lot#10; Cell Signaling Inc.) or amphiregulin (AREG) antibodies (1:100, cat# bs-3847R, lot# AH10221226; Bioss Inc.) in a blocking buffer at 4°C overnight. After washing with PBS, cells were incubated with Alexa Fluor 488 goat anti-rabbit (1:300; Thermo Fisher Scientific) for 30 min at room temperature. Nuclei were visualized with DAPI (Invitrogen). Cross sections of lungs from all mice were used to count the number of thrombi and fibrin thrombi after H&E staining, and the average per section was used to compare the control group with the selumetinib treatment group. The number of lymphocytes, endothelial and bronchiolar epithelial cells were counted from the areas with bronchioles and blood vessels. The

ratios were calculated for comparison between the control group and the treatment group.

2.2.3 | Statistical analysis

Data were presented as mean ± SD. from at least three independent experiments. Statistical comparisons between two groups were performed using a two-tail unpaired t-test.[13] $p < 0.05$ was indicated as the statistically significant difference.

3 | RESULTS

Activation of mitogen-activated protein kinases (MAPKs), including $MEK^{1/2}$, represents critical signal transducers that respond to viral infection, resulting in alteration of cell functions, such as cell differentiation, proliferation, survival, and apoptosis.[14] Activation of physiological intracellular signaling cascades caused by SARS-CoV-2 infection may lead to the phosphorylation and activation of down-stream molecules, and specific inhibitors may help reduce SARS-CoV-2-induced symptoms. We examined $MEK^{1/2}$ activity by detecting $ERK^{1/2}$ phosphorylation in patients with SARS-CoV-2 infection. As indicated in Figure 1A, we detected a high level of $ERK^{1/2}$ phosphorylation in COVID-19 patients, suggesting that $MEK^{1/2}$ activation occurs in patients with COVID-19.

To test the role of $MEK^{1/2}$ activity in SARS-CoV-2-induced lung damage, we need to use a model system and a specific inhibitor. K18-hACE2 transgenic mice are susceptible to SARS-CoV-2 infection and are a commonly used mouse model for COVID-19.[15–17] We first tested whether SARS-CoV2 infection in K18-hACE2 transgenic mice causes activation of $MEK^{1/2}$, as indicated by $ERK^{1/2}$ phosphorylation. We monitored $ERK^{1/2}$ phosphorylation in the lung tissue following SARS-CoV2 infection and detected a high phosphorylated $ERK^{1/2}$ (Figure 1B,C).

To demonstrate that selumetinib is effective in suppressing $MEK^{1/2}$ activity, we examined the level of $ERK^{1/2}$ phosphorylation by immunofluorescent staining. Phospho-ERK was highly detectable in lung tissues following SARS-CoV-2 infection (Figure 1C). In contrast, selumetinib injection nearly diminished phospho-$ERK^{1/2}$ in the lung tissues (Figure 1D), indicating that selumetinib effectively suppresses $MEK^{1/2}$ activation.

We performed histological analyses and found significant differences between the selumetinib treatment group and the control group in the infected mice (Figure 2). Mice infected with SARS-CoV-2 exhibit chronic interstitial pneumonia, fibrin thrombi (indicated as # in Figure 2A), thrombi (indicated by ** in Figure 2B), perivascular and peribronchiolar lymphocytic infiltration (indicated by an orange * in Figure 2C), alveolar macrophages (see green arrows in Figure 2D), active bronchiolar epithelial cell degeneration (a green arrow in Figure 2B indicated degenerated cells). Collapsed alveoli were common in SARS-CoV-2 infected lung tissues (indicated by * in Figure 2A). With selumetinib treatment, the SARS-CoV-2 infected lung tissues looked essentially normal (Figure 2E–H), but contained multifocal lymphoid nodules. Thrombi and congestion were less severe in selumetinib-treated mice (shown in Figure 2E–H). We observed a significant reduction in the number of thrombi and fibrin thrombi in the seleumetinib treatment group (Figure 2I,J, with
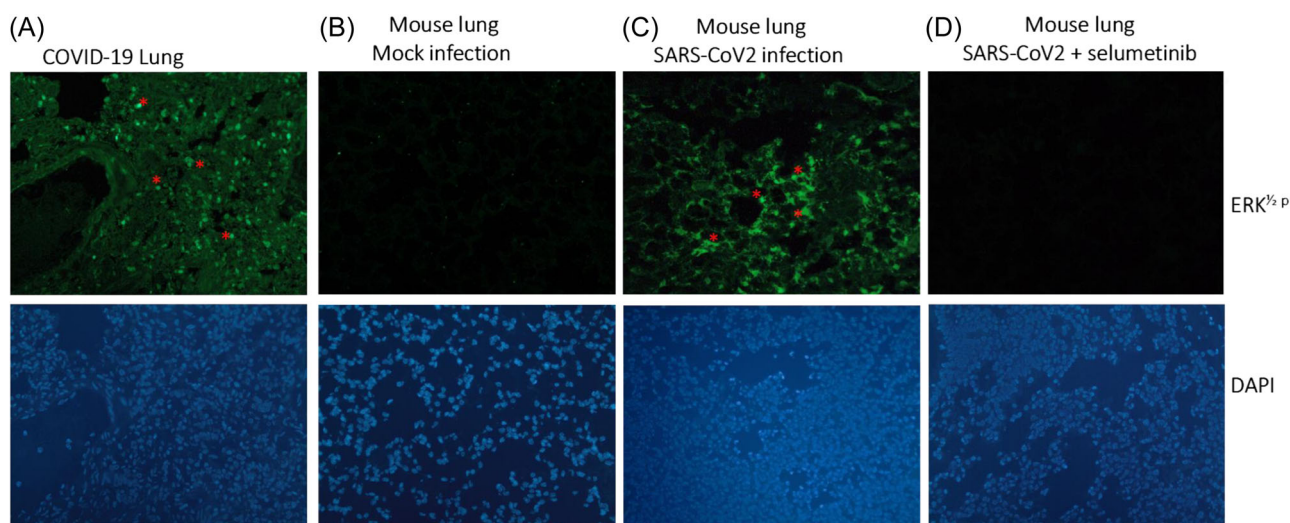

FIGURE 1 $ERK^{1/2}$ phosphorylation in SARS-CoV-2-infected lung tissues of mice and humans. $ERK^{1/2}$ phosphorylation was detected by immunofluorescent staining using specific antibodies (shown in green and highlighted in red*). Positive staining was observed in lung tissues from COVID-19 patients (A), SARS-CoV-2-infected K18-hACE2 transgenic mice (C), not in the lung tissues of mock-infected lung tissues (B). When K18-hACE2 transgenic mice were treated with MEK inhibitor selumetinib, ERK phosphorylation was not detectable (D), indicating effective suppression of MEK activity by selumetinib. $ERK^{1/2}$ phosphorylation was shown in red (top panels) and nuclear staining was done with DAPI (shown in blue, bottom panels). COVID-19, coronavirus disease 2019; DAPI, 4′,6-diamidino-2-phenylindole; ERK, extracellular signal-regulated kinase; MEK, mitogen-activated protein kinase; SARS-CoV-2, severe acute respiratory syndrome coronavirus 2.
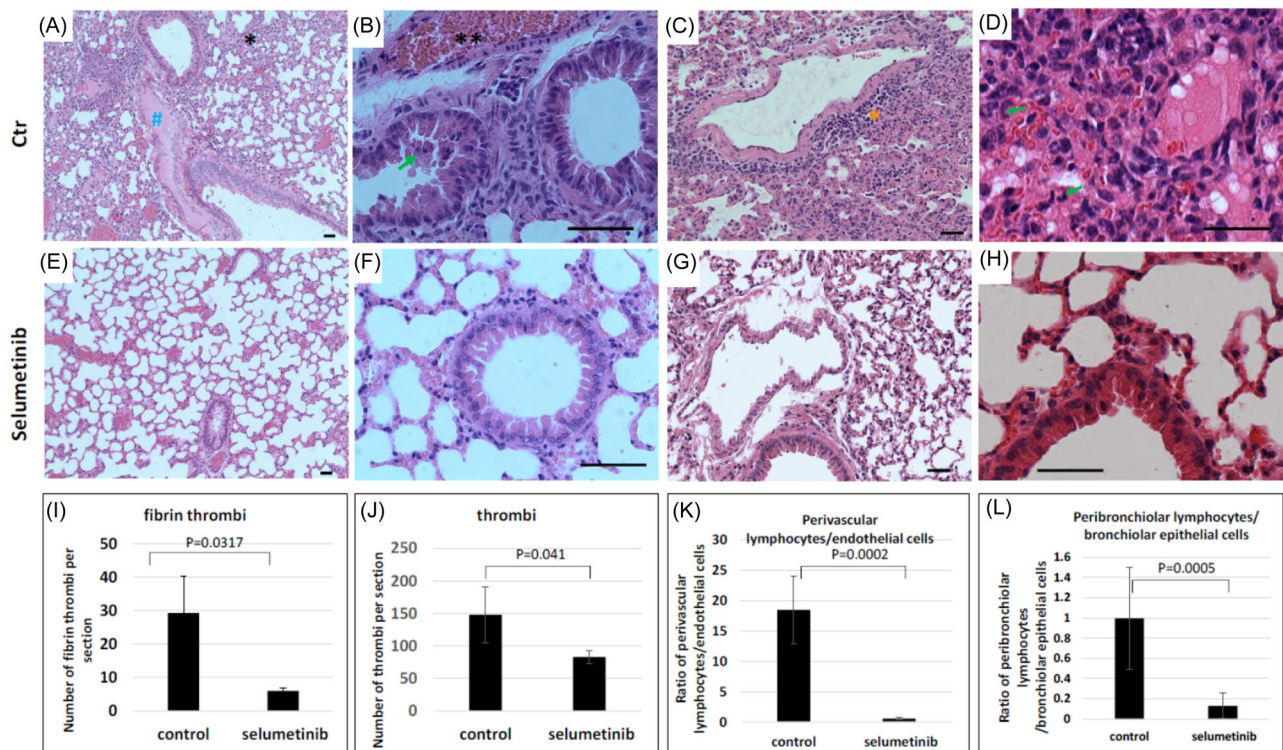
FIGURE 2 Histological changes of lung tissues by selumetinib. Hematoxylin and eosin slides were examined for changes in lung tissues. (A–D) were from the control group and (E–H) were from selumetinib treatment group. (I–L) are summaries of data analyses as described below. We detected fibrin thrombi (indicated by # in A), thrombi (indicated by ** in B) in SARS-CoV-2-infected mouse lung tissues. We also observed active bronchiolar epithelial cell degeneration (indicated by a green arrow in B), perivascular (indicated by red * in C) and peribronchiolar lymphocytic infiltration (shown in D), and collapsed alveoli (indicated by a * in A). All these symptoms were less severe in selumetinib-treated mice (as shown in E–H). We found that the number of fibrin thrombi (I) ($p = 0.0317$) and thrombi (J) ($p = 0.041$) per lung tissue section was significantly lower in selumetinib-treated mice. The biggest difference was the ratio of perivascular lymphocytes to endothelial cells between the control group and the selumetinib-treated group (K) ($p = 0.0002$). A lower ratio between peribronchiolar lymphocytes to bronchiolar epithelial cells was also observed between the control group and the selumetinib treatment group (L) ($p = 0.0005$). SARS-CoV-2, severe acute respiratory syndrome coronavirus 2.
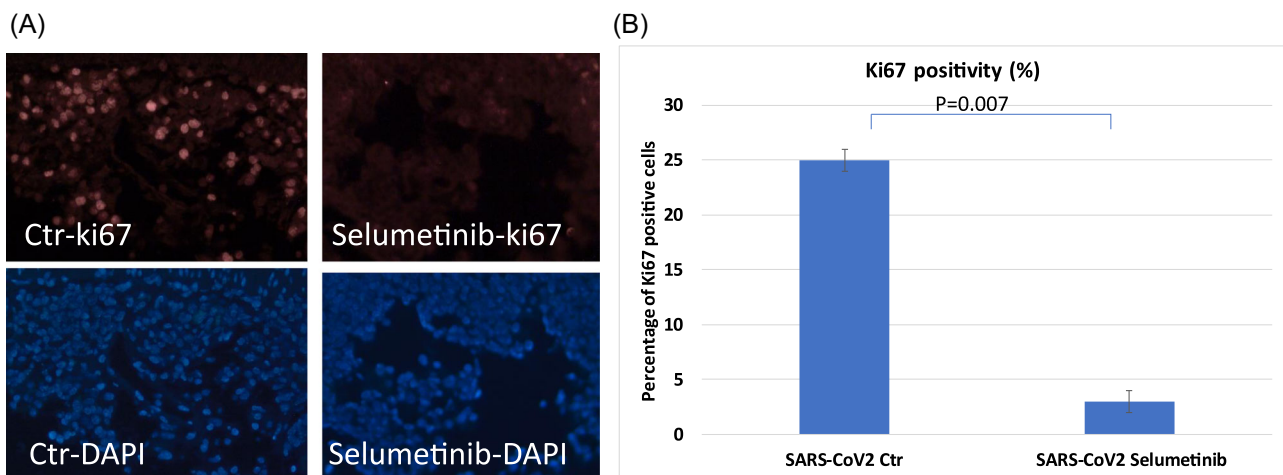

FIGURE 3 The efficacy of selumetinib on ki67 positivity of lung tissues from SARS-CoV-2 infected mice. (A) Typical images of Ki67 and DAPI staining. The presence of Ki67-positive cells (in red) was observed in SARS-CoV-2 infected K18-hACE2 mice, but only a few in selumetinib (shown as drug)-treated mice. (B) Summary of ki67 staining from three mice in each group. Three fields were counted from each mouse lung tissue and the number is the average from three mice/group. $p = 0.007$. DAPI, 4′,6-diamidino-2-phenylindole; SARS-CoV-2, severe acute respiratory syndrome coronavirus 2.

p values of 0.04 and 0.03 respectively). Similarly, the ratio of perivascular lymphocytes to endothelial cells in the areas with blood vessels was significantly lower in selumetinib-treated mice (Figure 2K, $p = 0.0002$). Samples from selumetinib treatment group also have a significantly lower ratio of peribronchiolar lymphocytes to bronchiolar epithelial cells (Figure 2L, $p = 0.0005$). These data strongly indicate that selumetinib reduces SARS-CoV-2-induced lung tissue damage.

It is known that MEK[1/2] plays an essential role in cell proliferation, and nuclear ki67 expression is a marker for cell proliferation.[14] After immunofluorescent staining with ki67 antibodies, we observed >25% of ki67 positivity in SARS-CoV-2 infected lung tissues. After selumetinib treatment, ki67 positivity was reduced to <5% ($p = 0.007$) (Figure 3). This result suggests that selumetinib reduces cell proliferation in the infected lung tissue. Further examination suggested that ki67-positive cells are mostly lymphocytes.

Next, we determined whether selumetinib effectively reduces mouse mortality after SARS-CoV-2 infection. In the K18-hACE2 mouse model, most mice die on Days 5–7 after virus infection. We observed a tendency for better survival for mice treated with selumetinib. On Day 11, we found that the survival rate of the mice treated with selumetinib was twice that of the control mice (67% vs. 33%). This result suggests that selumetinib may be effective in reducing COVID-19-related mortality.

There are numerous mechanisms by which MEK[1/2] is activated, including activation of upstream growth factors and signaling crosstalk. We detected elevated expression of the growth factor AREG in SARS-CoV2-infected mouse lung tissues compared with mock-infected tissues (see Figure 4). This result suggests that elevated AREG expression may be partly responsible for MEK[1/2] activation in the lung tissues after SARS-CoV2 infection.

From these data, we conclude that MEK[1/2] inhibitor selumetinib effectively reduces SARS-CoV-2 infection-induced lung damage and could be repurposed to treat COVID-19 patients.

4 | DISCUSSION

This study identified MEK[1/2] as a targetable vulnerability for SARS-CoV-2-induced symptoms in a mouse model of COVID-19. The MEK[1/2] inhibitor selumetinib is well-tolerated in cancer patients, with very low toxicity. In fact, selumetinib has been approved by FDA to treat uveal melanoma, NF1-related inoperable plexiform neurofibromas, and subsets of liver cancer and acute myeloid leukemia. Our data indicate that selumetinib could be repurposed to treat COVID-19 patients to reduce SARS-CoV-2-induced symptoms, including long haulers. While our studies provide insightful information on how SARS-CoV-2 induces lung damage, we anticipate more in-depth studies will follow. In addition to mechanistic studies, there are several strategies available to block SARS-CoV-2-induced activation of the AREG-MEK signaling axis, such as neutralizing antibodies against AREG, RAF, and MEK inhibitors. We also anticipate that alternatives to the K18-hACE2 transgenic mice may be useful for a better understanding of the pathological process of SARS-CoV-2 infection.
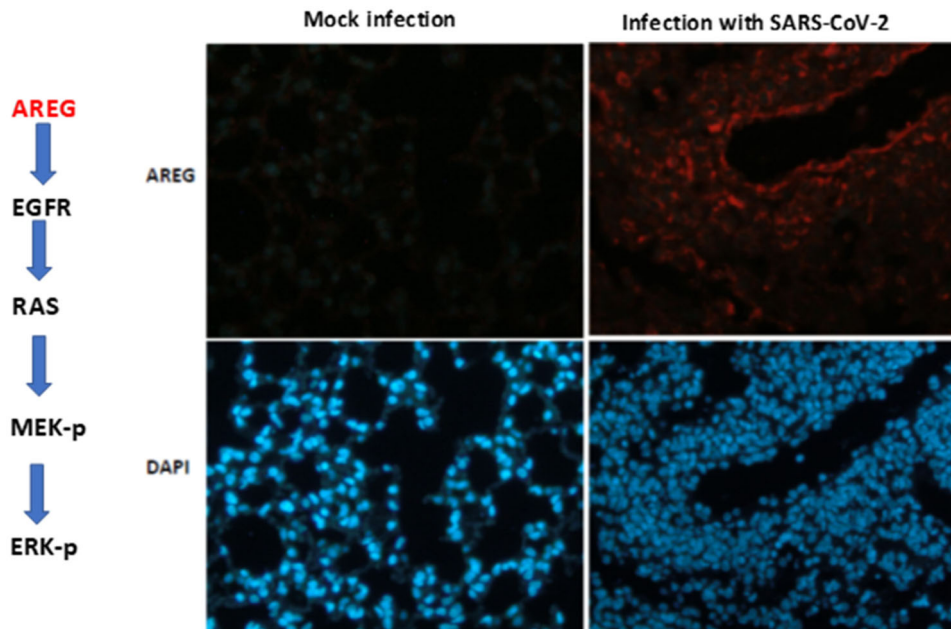

FIGURE 4 Detection of amphiregulin (AREG) expression in K18hACE2 transgenic mice with or without SARS-CoV-2 infection. AREG protein was detected by immunofluorescent staining (shown in red) with specific antibodies. No AREG expression was observed in mock-infected mouse lung tissues, whereas high expression of AREG was seen in SARS-CoV-2- infected mouse lung tissues. DAPI, 4′,6-diamidino-2-phenylindole; EGFR, epidermal growth factor receptor; ERK, extracellular signal-regulated kinase; MEK, mitogen-activated protein kinase; SARS-CoV-2, severe acute respiratory syndrome coronavirus 2.

The relevance of this study to human COVID-19 may be further studied using the real-world data from the Optum data set.

This study has limitations. All mouse studies used only one mouse model. Although K18-hACE2 mice are a commonly used model for studying COVID-19 pathogenesis, they do not exactly represent all the symptoms of human COVID-19.

AUTHOR CONTRIBUTIONS

Jingwu Xie: conceptualization, data collection, data analysis, and manuscript writing. **Michael J. Klemsz**: methodology, and manuscript review. **Melissa A. Kacena**: data collection, and manuscript review. **George Sandusky**: data collection and manuscript review. **Xiaoli Zhang**: conceptualization, methodology, data collection, and analyses. **Mark H. Kaplan**: methodology review, resources, and manuscript review.

ACKNOWLEDGMENTS

CONFLICT OF INTEREST

The authors declare no conflict of interest.

DATA AVAILABILITY STATEMENT

Data sharing is not applicable to this article as no new data were created or analyzed in this study.

REFERENCES

1. Gandhi RT, Lynch JB, Del Rio C. Mild or moderate Covid-19. *N Engl J Med*. 2020;383(18):1757-1766.
2. Berlin DA, Gulick RM, Martinez FJ. Severe Covid-19. *N Engl J Med*. 2020;383(25):2451-2460.
3. Parker AM, Brigham E, Connolly B, et al. Addressing the post-acute sequelae of SARS-CoV-2 infection: a multidisciplinary model of care. *Lancet Respir Med*. 2021;9(11):1328-1341.
4. Groff D, Sun A, Ssentongo AE, et al. Short-term and long-term rates of postacute sequelae of SARS-CoV-2 infection: a systematic review. *JAMA Netw Open*. 2021;4(10):e2128568.
5. Schumann M, Dobbelstein M. Adenovirus-induced extracellular signal-regulated kinase phosphorylation during the late phase of infection enhances viral protein levels and virus progeny. *Cancer Res*. 2006;66(3):1282-1288.
6. Andrade AA, Silva PN, Pereira AC, et al. The vaccinia virus-stimulated mitogen-activated protein kinase (MAPK) pathway is required for virus multiplication. *Biochem J*. 2004;381(pt 2):437-446.
7. Schrader T, Dudek SE, Schreiber A, Ehrhardt C, Planz O, Ludwig S. The clinically approved MEK inhibitor trametinib efficiently blocks influenza A virus propagation and cytokine expression. *Antiviral Res*. 2018;157:80-92.
8. Laure M, Hamza H, Koch-Heier J, et al. Antiviral efficacy against influenza virus and pharmacokinetic analysis of a novel MEK-inhibitor, ATR-002, in cell culture and in the mouse model. *Antiviral Res*. 2020;178:104806.
9. Schreiber A, Viemann D, Schöning J, et al. The MEK1/2-inhibitor ATR-002 efficiently blocks SARS-CoV-2 propagation and alleviates pro-inflammatory cytokine/chemokine responses. *Cell Mol Life Sci*. 2022;79(1):65.
10. Santry LA, Ingrao JC, Yu DL, et al. AAV vector distribution in the mouse respiratory tract following four different methods of administration. *BMC Biotechnol*. 2017;17(1):43.
11. Awosanya OD, Dalloul CE, Blosser RJ, et al. Osteoclast-mediated bone loss observed in a COVID-19 mouse model. *Bone*. 2022;154:116227.
12. Song R, Gu D, Zhang L, et al. Functional significance of Hippo/YAP signaling for drug resistance in colorectal cancer. *Mol Carcinog*. 2018;57(11):1608-1615.
13. Li J, Gu D, Lee SS, et al. Abrogating cholesterol esterification suppresses growth and metastasis of pancreatic cancer. *Oncogene*. 2016;35(50):6378-6388.
14. Whitmarsh AJ, Davis RJ. A central control for cell growth. *Nature*. 2000;403(6767):255-256.
15. Winkler ES, Bailey AL, Kafai NM, et al. SARS-CoV-2 infection of human ACE2-transgenic mice causes severe lung inflammation and impaired function. *Nat Immunol*. 2020;21(11):1327-1335.
16. Bao L, Deng W, Huang B, et al. The pathogenicity of SARS-CoV-2 in hACE2 transgenic mice. *Nature*. 2020;583(7818):830-833.
17. Oladunni FS, Park JG, Pino PA, et al. Lethality of SARS-CoV-2 infection in K18 human angiotensin-converting enzyme 2 transgenic mice. *Nat Commun*. 2020;11(1):6122.